

# RSC Advances



This is an *Accepted Manuscript*, which has been through the Royal Society of Chemistry peer review process and has been accepted for publication.

*Accepted Manuscripts* are published online shortly after acceptance, before technical editing, formatting and proof reading. Using this free service, authors can make their results available to the community, in citable form, before we publish the edited article. This *Accepted Manuscript* will be replaced by the edited, formatted and paginated article as soon as this is available.

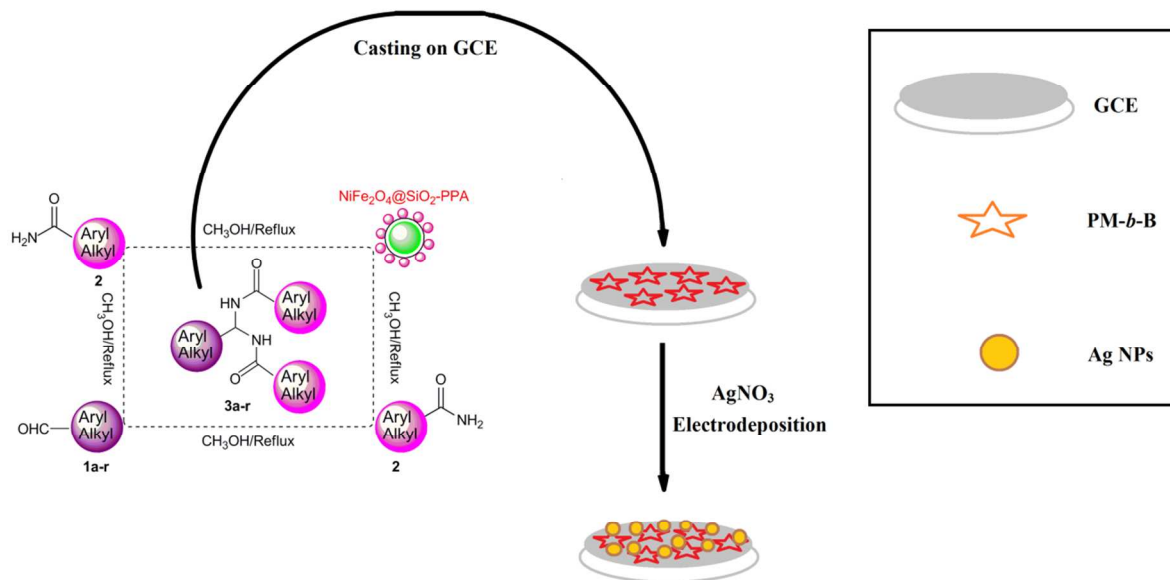
You can find more information about *Accepted Manuscripts* in the [Information for Authors](#).

Please note that technical editing may introduce minor changes to the text and/or graphics, which may alter content. The journal's standard [Terms & Conditions](#) and the [Ethical guidelines](#) still apply. In no event shall the Royal Society of Chemistry be held responsible for any errors or omissions in this *Accepted Manuscript* or any consequences arising from the use of any information it contains.

## Graphical Abstract

Synthesis of symmetrical *N,N'*-alkylidene *bis*-amides catalyzed by silica coated magnetic  $\text{NiFe}_2\text{O}_4$  nanoparticles supported polyphosphoric acid ( $\text{NiFe}_2\text{O}_4@\text{SiO}_2\text{-PPA}$ ) and its application toward silver nanoparticle synthesis for electrochemical detection of glucose

Behrooz Maleki, Mehdi Baghayeri



- For the first time, the synthesized *N,N'*-(phenylmethylene)-bis-benzamide (PM-*b*-B) has been used as a base for electrochemical deposition of silver nanoparticles to fabricate  $\text{Ag}@$ PM-*b*-B nanocomposite.
- The  $\text{Ag}@$ PM-*b*-B nanocomposite showed high affinity to sensitive detection of glucose as a novel sensor.
- The supported catalyst could be recycled and reused with the simple application of an external magnetic field, while retaining similar catalytic activity for six successive reactions.

**Synthesis of symmetrical *N,N'*-alkylidene *bis*-amides catalyzed by silica coated magnetic NiFe<sub>2</sub>O<sub>4</sub> nanoparticles supported polyphosphoric acid (NiFe<sub>2</sub>O<sub>4</sub>@SiO<sub>2</sub>-PPA) and its application toward silver nanoparticle synthesis for electrochemical detection of glucose**

**Behrooz Maleki\*, Mehdi Baghayeri**

*Department of Chemistry, Hakim Sabzevari University, Sabzevar, 96179-76487, Iran*

*E-mail: b.maleki@hsu.ac.ir, Tel: +98-44013324 Fax: +98-514401300*

**Abstract**

A green and efficient procedure for the synthesis of *N,N'*-alkylidene *bis*-amide derivatives has been developed by one-pot condensation of aldehydes and amides in the presence of a magnetic supported acid catalyst NiFe<sub>2</sub>O<sub>4</sub>@SiO<sub>2</sub>-PPA (NFS-PPA) as a highly effective heterogeneous catalyst under solvent-free conditions in refluxing methanol. The magnetically recoverable catalyst was easily recycled at least six times without significant loss of catalytic activity. We report on the modification of a glassy carbon electrode with *N,N'*-(phenylmethylene)-*bis*-benzamide (PM-*b*-B), and how this electrode can serve as a platform for the construction of Ag nanoparticles as a novel electrochemical sensor for glucose detection.

**Keywords:** Nanomagnetic catalyst, *N,N'*-Alkylidene *bis*-amide, Heterogeneous catalyst, Electrochemical sensor, Glucose

## Introduction

Amides are widely used not only in chemical industries but also in organic synthesis. Specifically, bisamides are key fragments for the introduction of *gem*-diaminoalkyl residues in retro-inverse pseudopeptide derivatives.<sup>1,2</sup> These compounds are synthesized by the condensation of aldehydes and amides using catalysts such as sulfuric acid,<sup>3</sup> trifluoromethanesulfonic acid (CF<sub>3</sub>SO<sub>3</sub>H),<sup>4</sup> sulfamic acid (NH<sub>2</sub>SO<sub>3</sub>H),<sup>5</sup> *p*-toluenesulfonic acid (*p*-TSA),<sup>6</sup> silica-supported barium chloride (SiO<sub>2</sub>-BaCl<sub>2</sub>),<sup>7</sup> boric acid [B(OH)<sub>3</sub>],<sup>8</sup> phosphotungstic acid (PWA),<sup>9</sup> silica-supported perchloric acid (HClO<sub>4</sub>-SiO<sub>2</sub>),<sup>10</sup> silica-supported polyphosphoric acid (SiO<sub>2</sub>-PPA),<sup>11</sup> silica-supported magnesium chloride (SiO<sub>2</sub>-MgCl<sub>2</sub>),<sup>12</sup> and *tris*(hydrogensulfato)boron [B(HSO<sub>4</sub>)<sub>3</sub>],<sup>13</sup> nano-SnCl<sub>4</sub>.SiO<sub>2</sub>,<sup>14</sup> and H<sub>14</sub>[NaP<sub>5</sub>W<sub>29</sub>MoO<sub>110</sub>].<sup>15</sup> However, several of these methods suffer from some drawbacks such as prolonged reactions times, unsatisfactory yield, utilization of hazardous organic solvents, tedious work-up conditions, use of microwave irradiation, employment of large amounts of catalyst and harsh reaction conditions. The present work reports the use of polyphosphoric acid supported on silica-coated NiFe<sub>2</sub>O<sub>4</sub> nanoparticle (NiFe<sub>2</sub>O<sub>4</sub>@SiO<sub>2</sub>-PPA) as a catalyst for the preparation of symmetrical *N,N'*-alkylidene *bis*-amides.

In recent years, there has been a rapid growth in the development of novel supported compounds such as supported catalysts, reagents and scavengers. Preparing heterogeneous catalysts by immobilizing the homogenous precursors on solid support is one of the important routes for developing novel heterogeneous catalysts. In most of these cases, the immobilized catalysts so prepared could provide advantages over their unsupported counterparts in terms of easy separation, low toxicity, moisture resistance, air tolerance, easy handling, reusability.<sup>16-18</sup>

On a different note, magnetic nanoparticles (MNPs) have gained an increasing interest because

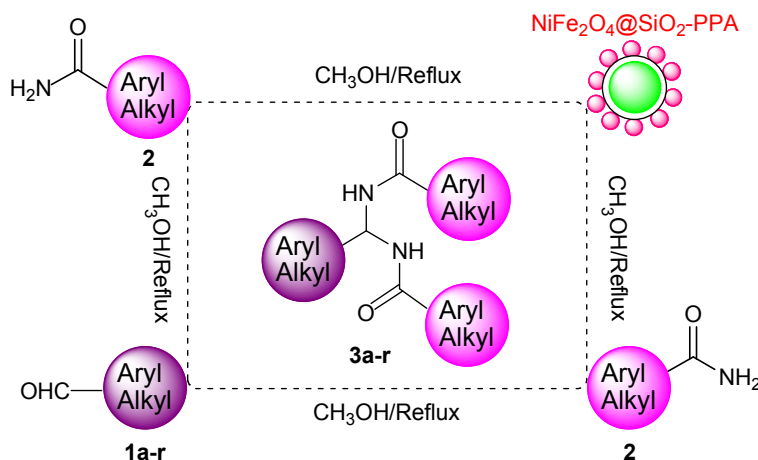
of their potential applications such as their uses for cell separation,<sup>19</sup> magnetic resonance imaging,<sup>20</sup> drug delivery systems,<sup>21</sup> protein separation<sup>22</sup> and cancer treatments through hyperthermia.<sup>23</sup> Also, magnetic nanoparticles (MNPs) can be a good candidate as a support material for heterogeneous catalysts, because of easy synthesis, high surface area, facile separation by magnetic forces, and low toxicity and cost.<sup>24</sup> According to these attractive properties, many MNPs supported catalysts have been designed and widely applied as novel magnetically separated catalysts in traditional metal catalysis,<sup>25</sup> organocatalysis,<sup>26</sup> and even enzyme catalysis.<sup>27</sup>

Material selection process is of paramount importance to achieve successful low-cost engineering design that can fit functional requirements as well as customer satisfaction attributes for various sensing applications. This is usually carried out considering various conflicting criteria and utilizing decision making tools to reveal the potential of new materials in expanding the possibilities of new applications. In recent years, MNPs have been a center of scientific interest and active multidisciplinary research because of their excellent potential for widespread applications such as rechargeable batteries, sensors, electro-catalyst and so on.<sup>28</sup> The ability to precisely prepare MNPs on a large scale with tailored morphology and geometry is an important goal of the material science. In the last decade, various methods have been developed to prepare high-density and well-aligned MNPs. The conventional techniques used to fabricate nanowires array include sol-gel method, chemical vapor deposition, direct electrodeposition and so forth. Among these methods, carrier-assisted electrodeposition has been established to be an attractive route for the synthesis of MNPs because of its simplicity, cost-effectiveness, low temperature fabrication, etc.<sup>29-30</sup> Also, the morphology, nanostructure, and composition of MNPs could be tuned through selectively controlling deposition parameters. Among them, the functional groups

on carriers play a crucial role in enhancing the formation of MNPs and its further applications.<sup>31</sup> Amino, carbonyl, carboxylic and thiol groups are the four types of functional groups most commonly used during the nanoparticle synthesis process; these functional groups can form stable recognition sites and cavities within their matrix. In this study, we have combined the advantages of the functional groups from the *N,N'*-(phenylmethylene)-bis-benzamide (**3a**) and the high ability of the electrodeposition technique to synthesis silver NPs. Beside this purpose, a glucose sensor based on a glassy carbon electrode coated with an *N,N'*-(phenylmethylene)-bis-benzamide and Ag NPs (Ag@PM-*b*-B/GCE) with a satisfactory selective recognition ability toward glucose have been prepared.

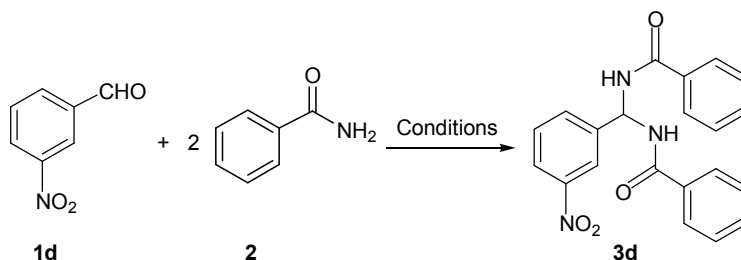
## Results and Discussion

As a continuation of our work on the development of efficient and environmentally benign reagents and catalysts,<sup>32</sup> we now report that NiFe<sub>2</sub>O<sub>4</sub>@SiO<sub>2</sub>-PPA is an excellent catalyst for the synthesis of symmetrical *N,N'*-alkylidene *bis*-amide derivatives (Scheme 1).



**Scheme 1.** Synthesis of symmetrical *N,N'*-alkylidene *bis*-amide.

In order to explore the catalytic activity of  $\text{NiFe}_2\text{O}_4@\text{SiO}_2\text{-PPA}$ ,<sup>33</sup> the condensation of 3-nitrobenzaldehyde (1 mmol) with benzamide (2 mmol) was selected as a model reaction (Scheme 2).



**Scheme 2.** The selected model reaction for synthesis of *N,N'*-(3-nitrophenylmethylene)dibenzamide (**3d**)

The effect of various parameters, such as the influence of solvents, concentration of the catalyst and temperature, was evaluated to optimize the reaction conditions (Table 1, entries 1-12). Additionally, this reaction took place in the absence of solvent using 0.1 g of catalyst at 110 °C and the yield (64%) in 50 min was achieved (entry 8). As can be seen from Table 1, the shortest time and best yield were achieved using 0.1 g of  $\text{NiFe}_2\text{O}_4@\text{SiO}_2\text{-PPA}$  (entry 2). It was found that by decreasing the catalyst amount from 0.1 to 0.08 and 0.05 g, the yield of the reaction decreased from 92 to 84 and 80 % (entries 9-10). When the amount of the catalyst increased from 0.1 to 0.12 and 0.24 g, there was no prominent change in the yield (entries 11-12). It is noteworthy that, in the absence of  $\text{NiFe}_2\text{O}_4@\text{SiO}_2\text{-PPA}$ , no product was detected in long reaction time (entry 13).

**Table 1** Various conditions used for the synthesis of *N,N'*-(3-nitroPhenylmethylene)dibenzamide (**3d**)

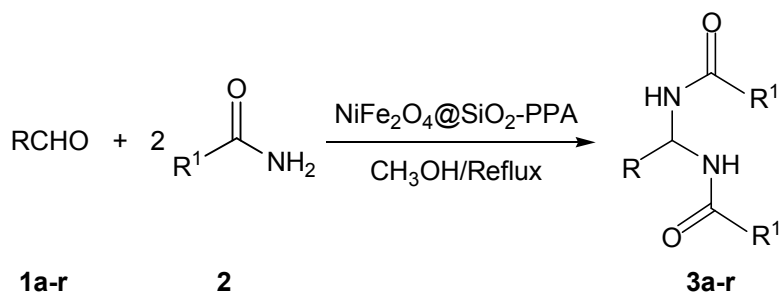
Entry	Catalyst (g)	Conditions	Time (min)	Yield (%)
1	NiFe <sub>2</sub> O <sub>4</sub> @SiO <sub>2</sub> -PPA (0.1 g)	Ethanol/reflux	50	83
2	NiFe <sub>2</sub> O <sub>4</sub> @SiO <sub>2</sub> -PPA (0.1 g)	Methanol/reflux	50	92
3	NiFe <sub>2</sub> O <sub>4</sub> @SiO <sub>2</sub> -PPA (0.1 g)	Ethyl acetate/reflux	50	50
4	NiFe <sub>2</sub> O <sub>4</sub> @SiO <sub>2</sub> -PPA (0.1 g)	Acetonitrile/Reflux	50	72
5	NiFe <sub>2</sub> O <sub>4</sub> @SiO <sub>2</sub> -PPA (0.1 g)	Toluene/reflux	50	83
6	NiFe <sub>2</sub> O <sub>4</sub> @SiO <sub>2</sub> -PPA (0.1 g)	Dichloromethane/reflux	50	32
7	NiFe <sub>2</sub> O <sub>4</sub> @SiO <sub>2</sub> -PPA (0.1 g)	1,4-Dioxane/reflux	50	84
8	NiFe <sub>2</sub> O <sub>4</sub> @SiO <sub>2</sub> -PPA (0.1 g)	Solvent-free/110 <sup>0</sup> C	50	64
9	NiFe <sub>2</sub> O <sub>4</sub> @SiO <sub>2</sub> -PPA (0.08 g)	Methanol/reflux	50	84
10	NiFe <sub>2</sub> O <sub>4</sub> @SiO <sub>2</sub> -PPA (0.05 g)	Methanol/reflux	50	80
11	NiFe <sub>2</sub> O <sub>4</sub> @SiO <sub>2</sub> -PPA (0.12 g)	Methanol/reflux	50	92
12	NiFe <sub>2</sub> O <sub>4</sub> @SiO <sub>2</sub> -PPA (0.24 g)	Methanol/reflux	50	92
13	-- <sup>a</sup>	Methanol/reflux	180	-- <sup>b</sup>

<sup>a</sup>In the absence of any catalyst. <sup>b</sup>No reaction.

To assess the efficiency and the scope of the nanomagnetic catalyst in the preparation of symmetrical *N,N'*-alkylidene *bis*-amides, the condensation of benzamide with a wide variety of aromatic aldehydes containing both electron-withdrawing and electron-donating groups and of aliphatic aldehydes was examined in the presence of NiFe<sub>2</sub>O<sub>4</sub>@SiO<sub>2</sub>-PPA in methanol under reflux condition (Table 2, entries 1-15). The method was also successfully worked when acetamide was used instead of benzamide in the reaction (Table 2, entries 16-18).

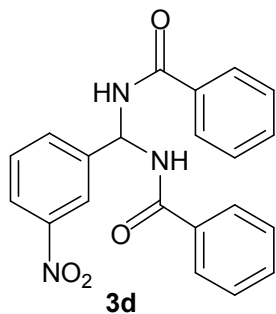


**Table 2** Synthesis of symmetrical *N,N'*-alkylidene *bis*-amide derivatives in the presence of NiFe<sub>2</sub>O<sub>4</sub>@SiO<sub>2</sub>-PPA

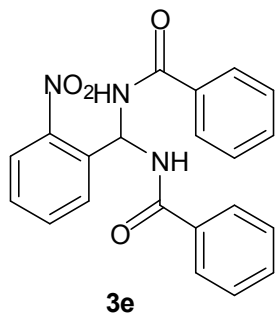


Entry	Products ( <b>3a-r</b> )	Yield <sup>a</sup> (%)	Time (min)	mp ( <sup>o</sup> C)	
				Found	Lit.
1	<p style="text-align: center;"><b>3a</b></p>	86	80	213-215	214-216 (Ref. 14)
2	<p style="text-align: center;"><b>3b</b></p>	92	40	257-259	259-261 (Ref. 14)
3	<p style="text-align: center;"><b>3c</b></p>	93	40	234-236	230-234 (Ref. 8)

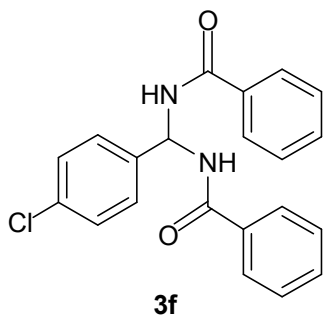
4 92 50 226-228 232-235 (Ref. 13)



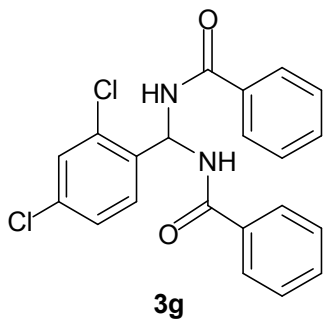
5 80 70 257-259 257-259 (Ref. 12)

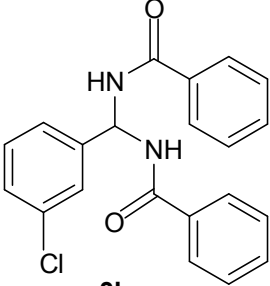
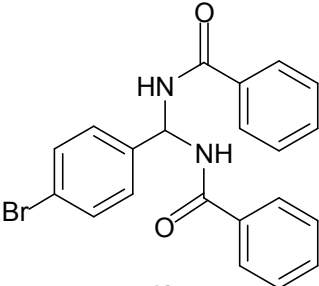
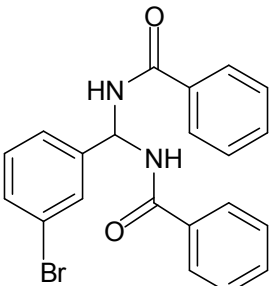
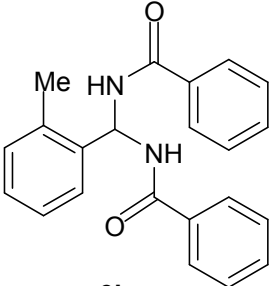


6 86 60 250-252 251-254 (Ref. 12)

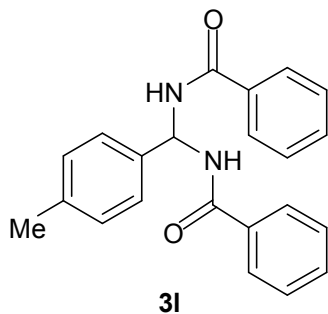


7 83 70 198-200 195-197 (Ref. 13)



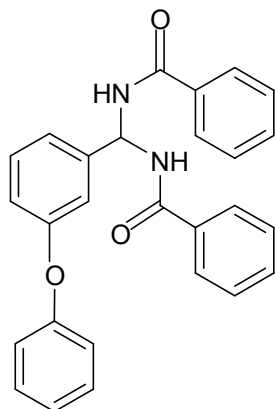
8	 <b>3h</b>	82	80	219-221	221-222 (Ref. 15)
9	 <b>3i</b>	90	60	254-256	252-254 (Ref. 13)
10	 <b>3j</b>	84	80	224-226	226-228 (Ref. 15)
11	 <b>3k</b>	75	100	220-222	223-225 (Ref. 15)

12 79 90 242-244 242-243 (Ref. 13)



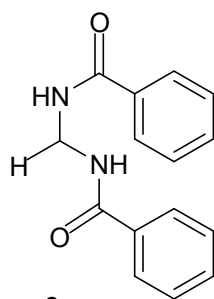
**3l**

13 90 50 192-193 194-196 (Ref. 15)



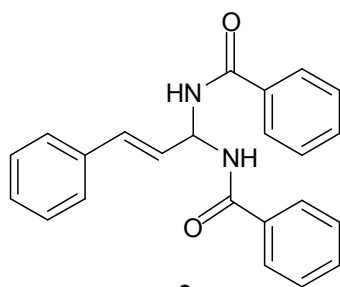
**3m**

14 71 100 217-219 216-218 (Ref. 10)

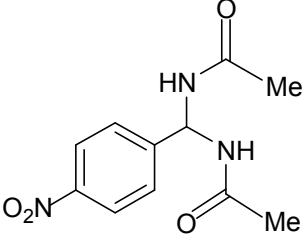
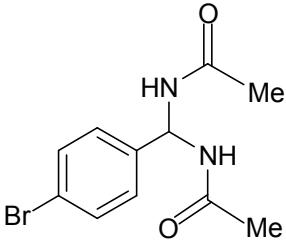
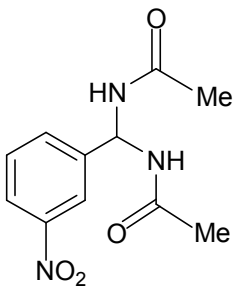


**3n**

15 52 130 200-202 199-201 (Ref. 14)



**3o**

16		90	60	270-272	270-272 (Ref. 10)
	<b>3p</b>				
17		82	80	243-245	244-246 (Ref. 10)
	<b>3q</b>				
18		85	60	230-232	231-233 (Ref. 6)
	<b>3r</b>				

<sup>a</sup>Isolated yields.

The recycling of NiFe<sub>2</sub>O<sub>4</sub>@SiO<sub>2</sub>-PPA was investigated using the synthesis of **3d**. After completion of the reaction, the nanomagnetic catalyst was separated from the reaction mixture by employing an external magnetic field, washed with acetone and dried at 100 °C for 2h. It was re-used directly in the model reaction to give **3d** in yields of 92%, 91%, 91%, 90%, 88%, 85%, 85%, 83%, 82%, and 80% for ten consecutive runs after 50 min.

The FT-IR spectra of catalyst before use (fresh) and after reuse ten times (recovered) were studied. As shown in Fig. 1, the FT-IR spectrum of the recovered nanocatalyst showed which the structure of catalyst remained almost the same after ten-run reuse.

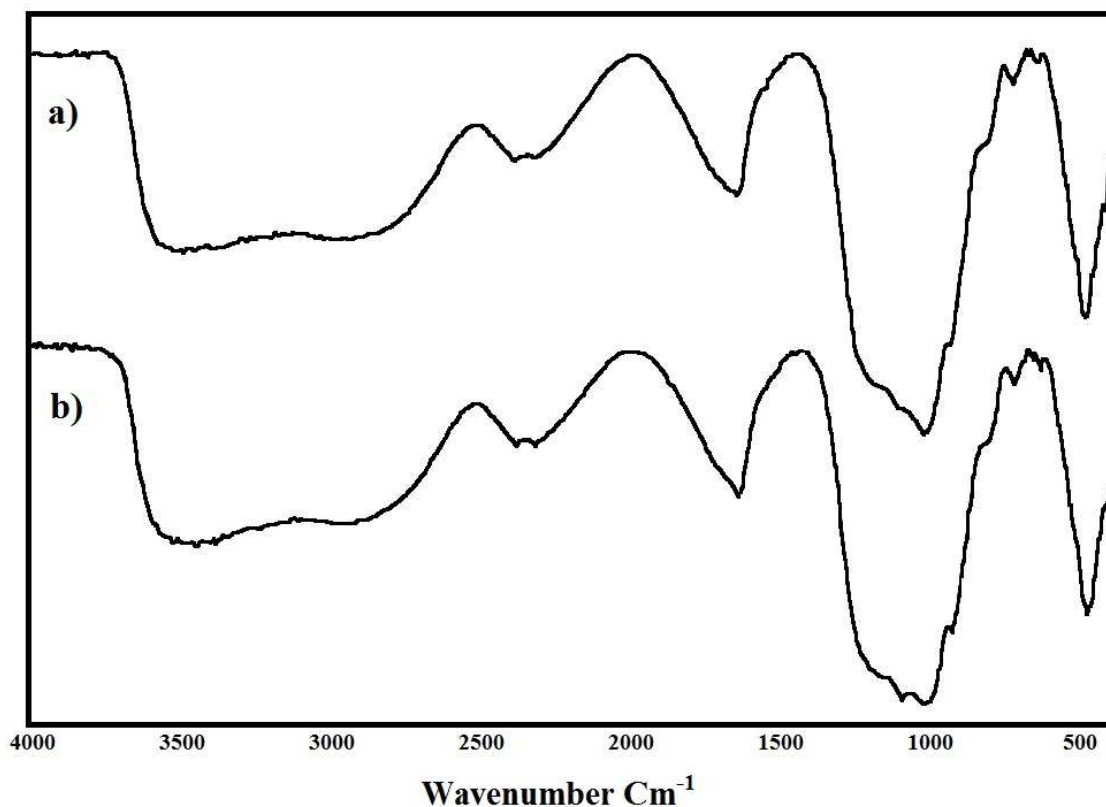
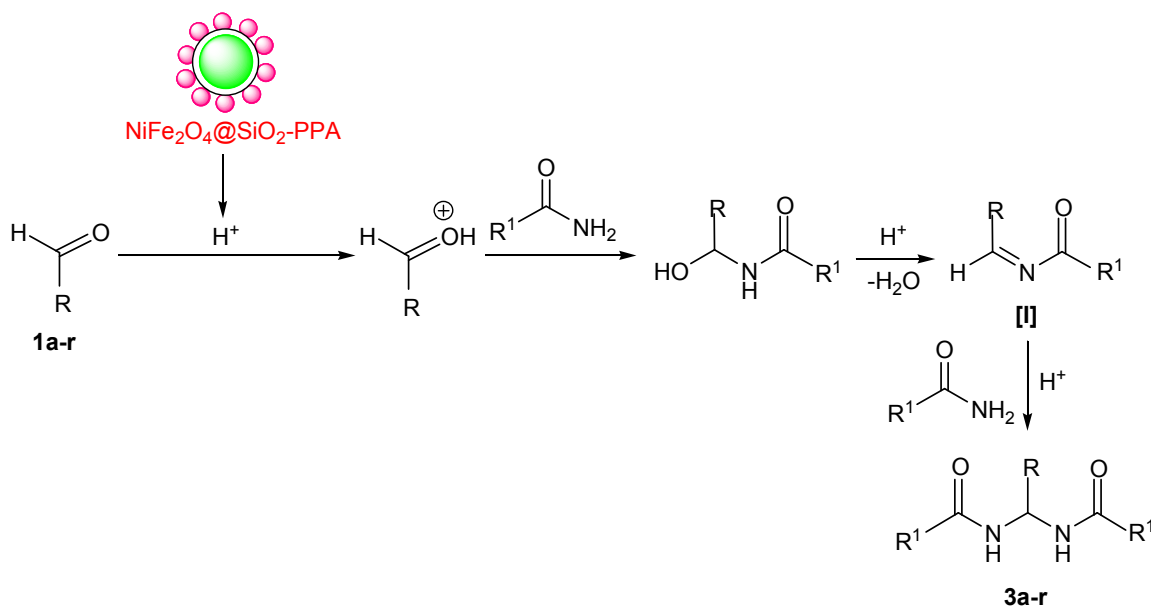


**Fig. 1.** FT-IR spectrum of (a) fresh and (b) recovered (after ten times)  $\text{NiFe}_2\text{O}_4@\text{SiO}_2\text{-PPA}$ .

As shown in Table 2, the aromatic aldehydes with electron-withdrawing groups reacted faster than the aromatic aldehydes with electron-donating groups. This observation can be rationalized on the basis of the mechanism in Scheme 3. The aldehyde is first activated by  $\text{NiFe}_2\text{O}_4@\text{SiO}_2\text{-PPA}$ . Nucleophilic addition of amides to activated aldehyde followed by loss of  $\text{H}_2\text{O}$  generates intermediate **I**, which is further activated by  $\text{NiFe}_2\text{O}_4@\text{SiO}_2\text{-PPA}$ . Then, nucleophilic addition of a

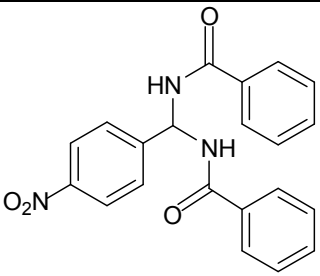
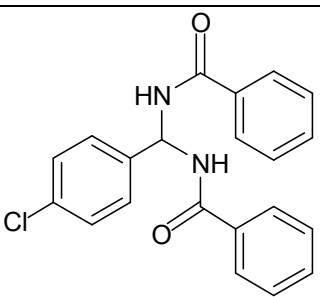
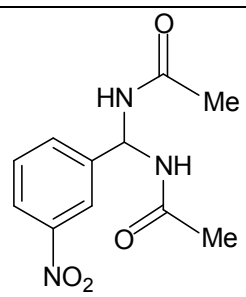
second molecule of amide to activated intermediate **I**, affords the symmetrical *N,N'*-alkylidene bisamide products (**3a-r**).



**Scheme 3.** Proposed mechanism

To test the worth of the present work in comparison with results in the literature, we compared results of NiFe<sub>2</sub>O<sub>4</sub>@SiO<sub>2</sub>-PPA with other applied Lewis and Bronsted acids in synthesis of *N,N'*-alkylidene *bis*-amides. These data, which are shown in Table 3, revealed that NiFe<sub>2</sub>O<sub>4</sub>@SiO<sub>2</sub>-PPA is a better catalyst than most of the conventional catalysts mentioned with respect to reaction times and yields of the obtained products.

**Table 3** Comparison of catalytic activity of NiFe<sub>2</sub>O<sub>4</sub>@SiO<sub>2</sub>-PPA with known catalysts in the synthesis of *N,N'*-alkylidene *bis*-amides

Entry	<i>N,N'</i> -Alkylidene <i>bis</i> -Amides	Conditions	Time (min)	Yield (%)
<b>3b</b>		SiO <sub>2</sub> -BaCl <sub>2</sub> /100 <sup>0</sup> C/solvent-free <sup>7</sup>	90	91
		B(OH) <sub>3</sub> /toluene/reflux <sup>8</sup>	1800	65
		PWA//toluene/reflux <sup>9</sup>	1200	71
		Present work	40	92
<b>3f</b>		B(OH) <sub>3</sub> /toluene/reflux <sup>8</sup>	2880	65
		SiO <sub>2</sub> -MgCl <sub>2</sub> /100 <sup>0</sup> C/solvent-free <sup>12</sup>	120	74
		H <sub>14</sub> [NaP <sub>5</sub> W <sub>29</sub> MoO <sub>110</sub> ]/methanol/reflux <sup>15</sup>	70	82
		Present work	60	86
<b>3r</b>		Sulfamic acid/125 <sup>0</sup> C/Solvent-Free <sup>5</sup>	1080	68
		H <sub>14</sub> [NaP <sub>5</sub> W <sub>29</sub> MoO <sub>110</sub> ]/methanol/reflux <sup>15</sup>	70	82
		Present work	60	85

Although the use of NiFe<sub>2</sub>O<sub>4</sub>@SiO<sub>2</sub>-PPA clearly shows that reaction times are better than some of the other methods in literature, the novelty and value of our results are principally related to comparison between homogeneous polyphosphoric acid (PPA) with heterogeneous novel NiFe<sub>2</sub>O<sub>4</sub>@SiO<sub>2</sub>-PPA. Polyphosphoric acid (PPA) suffers from drawbacks such as **a**) non-reusability and difficult separation, **b**) necessity to neutralize the reaction mixtures prior to



product isolation **c)** low stability, **d)** higher cost, **e)** higher toxicity and **f)** sensitivity to moisture and air. NiFe<sub>2</sub>O<sub>4</sub>@SiO<sub>2</sub>-PPA is easily separated by employing an external magnet and may be re-used without loss of activity. It is very stable, highly efficient due to its greater surface area and inexpensive because of the re-usability. Additionally, for the first time, a nanomagnetically separable catalyst (NiFe<sub>2</sub>O<sub>4</sub>@SiO<sub>2</sub>-PPA) has been used for the synthesis of *N,N'*-alkylidene bis-amides. Finally, we believe that the above points are the major advantages of our work compared to previous reports.

#### **The electrochemical characteristics of Ag@PM-*b*-B/GCE**

The oxidation–reduction behavior of Ag NPs on the surface of the GCE was estimated to attain direct and certain evidence for the formation of these nanoparticles. Cyclic voltammograms were recorded at the bare GCE, PM-*b*-B/GCE, and Ag@PM-*b*-B/GCE in phosphate buffer solution (PBS, pH 7.0), respectively, as shown in Fig. 2. As expected, no redox peaks were observed in the absence of Ag NPs. In contrast, when the Ag NPs were electrochemically deposited on the PM-*b*-B modified glassy carbon electrode surface, a clear anodic peak with a peak potential of +0.08 V vs. Ag|AgCl|KCl (3 M), which was the characteristic oxidation peak of Ag nanoparticles and a small reduction peak at potential of about -0.1 V vs. Ag|AgCl|KCl (3 M), which was related to the reduction of Ag<sup>+</sup> cations, appeared due to the excellent behavior of Ag NPs for the electron-transfer process.

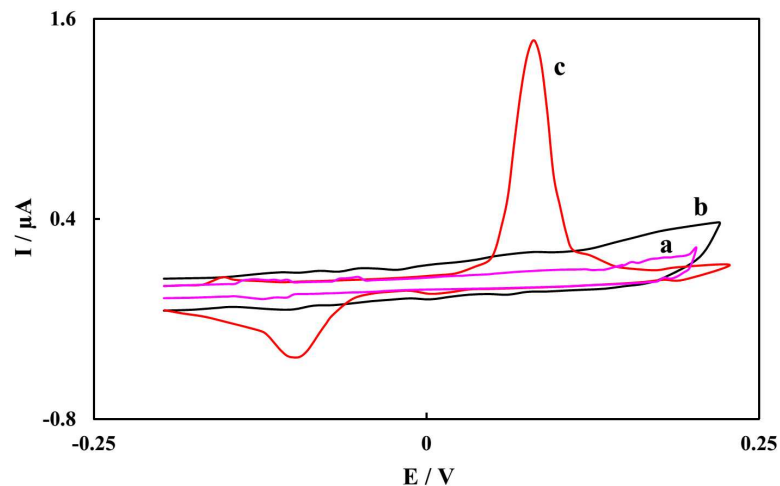


**Fig. 2.** Cyclic voltammogram of bare GCE (a), PM-*b*-B/GCE (b) and Ag@PM-*b*-B/GCE (c) in 0.1 M PBS (pH 7.0) at scan rate 100 mV s<sup>-1</sup>

The micro-morphology of Ag@PM-*b*-B film has been visualized by SEM images. As shown in Fig. 3a, the PM-*b*-B on the substrate presents a smooth and featureless morphology. After the electrodeposition of Ag NPs, it is obviously seen that many Ag nanoparticles are distributed and attached to the surface of the PM-*b*-B (Fig. 3b). As can be seen, the Ag film was composed of about 40 nm Ag NPs, and some Ag NPs assembled to large microspheres, which proves that the Ag NPs can definitely deposit on the PM-*b*-B modified surface and the Ag@PM-*b*-B interface is favorable for electron transfer and signal amplification.

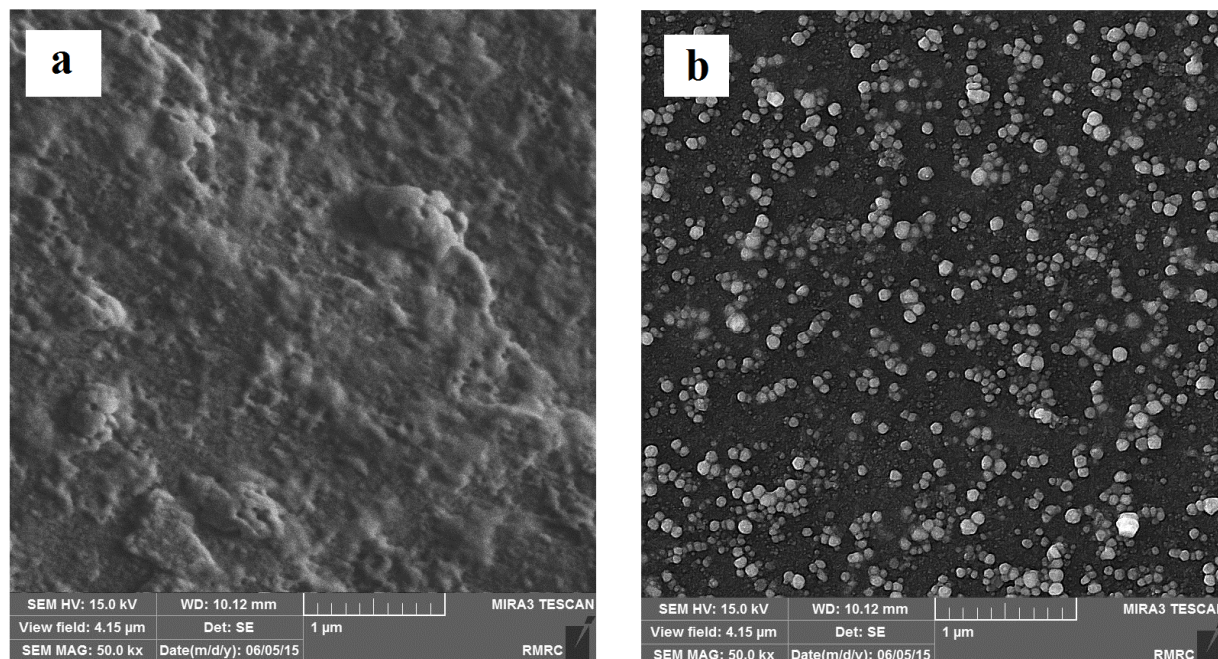


**Fig. 3.** The SEM images of (a) PM-*b*-B/GCE and (b) Ag@PM-*b*-B/GCE.

### Electrocatalytic oxidation of glucose

The electrocatalytic performance of the bare GCE, PM-*b*-B/GCE and Ag@PM-*b*-B/GCE toward the oxidation of glucose was investigated by CV. Fig. 4 describes the cyclic voltammograms of glucose (1 mM) on the bare GCE, PM-*b*-B/GCE and Ag@ PM-*b*-B/GCE in 0.1 M NaOH, respectively. The bare GCE (curve a) showed no electrochemical response in the presence of glucose, while a typical board oxidation peak was observed for PM-*b*-B/GCE (curve b) in the potential range from 0.4 to 1.15 V. However, after adding 1 mM glucose, Ag@PM-*b*-B/GCE (curve c) shows a notable catalytic current peak about 187 μA in intensity at 0.685 V. The excellent anodic peak current of glucose at surface of Ag@PM-*b*-B nanocomposite confirm that Ag@PM-*b*-B have high catalytic ability for glucose oxidation. The porous structure of Ag NPs on PM-*b*-B provide extra proper surface for improvement of their catalytic performance. All the

above explanations prove that Ag NPs contained in the nanocomposites present a remarkable catalytic performance for glucose oxidation.

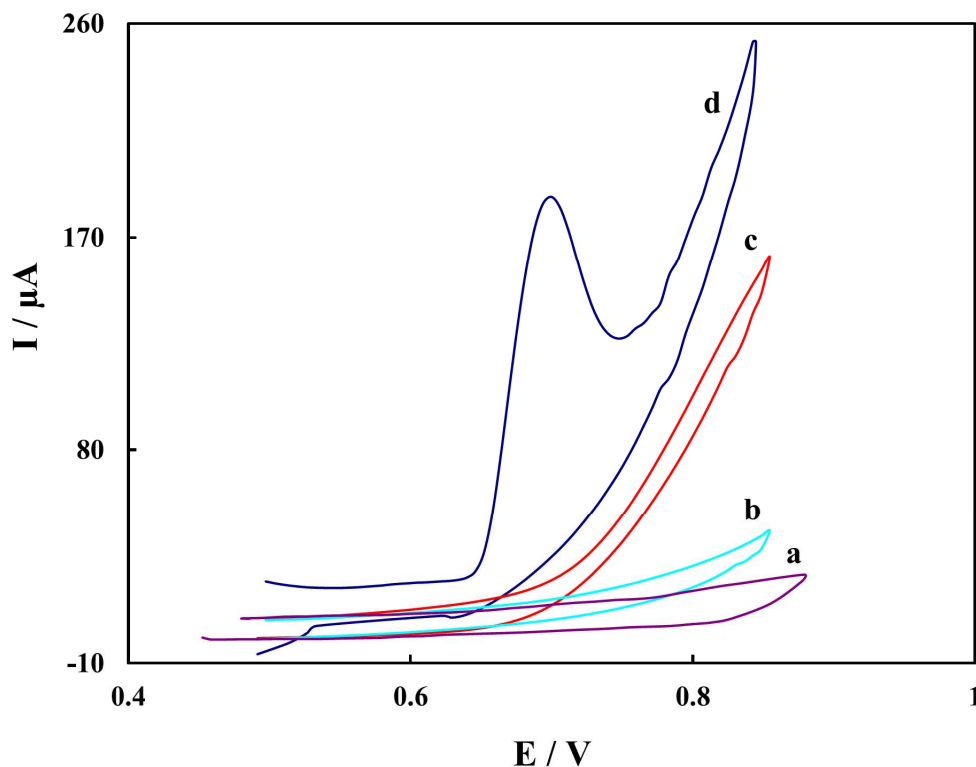


**Fig. 4.** Cyclic voltammogram of Ag@PM-*b*-B/GCE in absence of glucose (a) and cyclic voltammograms of 1 mM glucose in 0.1 M NaOH at the surface of different electrodes: bare GCE (b), PM-*b*-B/GCE (c) and Ag@PM-*b*-B/GCE (d) at scan rate of 100 mV s<sup>-1</sup>.

#### Amperometric response of the Ag@PM-*b*-B/GCE to glucose

Fig. 5A displays typical amperometric response of the Ag@PM-*b*-B/GCE to subsequent addition of glucose in alkaline solution at +0.7 V. It is perceived that the modified electrode responds quickly to the change of glucose concentration. With the successive additions of glucose, the response increases immediately and reaches 95% of the steady state value within 5 s. The corresponding calibration curve for the glucose sensor is shown in Fig. 5B. The sensor presents a linear range of 3-2000 μM with a detection limit of 1.4 μM (S/N = 3). Comparison of analytic performance for Ag@PM-*b*-B/GCE with other reported nonenzymatic glucose sensors is given

in Table 4. It can be observed that the performance of the present sensor is comparable or better than the other reported sensors. This may be related to the higher specific surface area of the deposited Ag nanoparticles which provides large surface-to-volume ratio and enhances active sites for the oxidation of glucose.

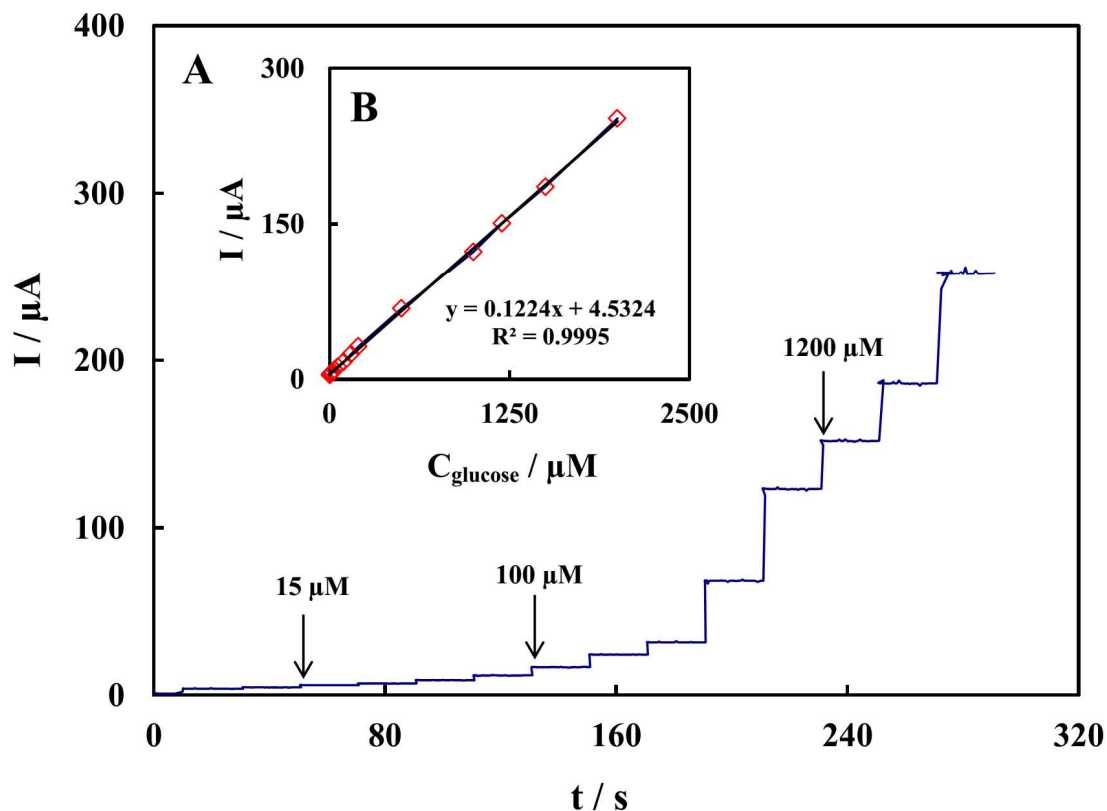


**Fig. 5.** (A) Typical amperometric response of the Ag@PM-b-B/GCE on successive injection of glucose into the stirring 0.1 M NaOH, applied potential: +0.7 V. (B) Calibration curve of glucose versus its concentration.

**Table 4** Comparison of analytic performance for Ag@PM-*b*-B/GCE with other reported nonenzymatic glucose sensors

Type of electrode	Detection limit ( $\mu\text{M}$ )	Linear range (mM)	Lit.
Pd-doped copper oxide nanofibers	190	0.0002–2.5	Ref. 34
Cu-Co NSs	10	0.015–1.21	Ref. 35
Ni-Cu/TiO <sub>2</sub> NTs	5	0.010–3.2	Ref. 36
5% NiO@Ag NWs	1.01	N/A	Ref. 37
Ti/TiO <sub>2</sub> nanotube array/Ni	4	0.1–1.7	Ref. 38
Ag@PM- <i>b</i> -B	1.4	0.003–2	This work

NWs: nanowires, NSs: nanostructures, NTs: nanotube arrays.

### Sensor stability and interference

The stability of Ag@PM-*b*-B/GCE was evaluated by amperometric measurement under a constant potential of +0.7 V for 1000 s. Fig. 6A shows relationship of the current responses and time for fabricated sensor. After 1000 s, Ag@PM-*b*-B/GCE keeps 76.44% quantity of initial current values, representing the high electrocatalytic stability and excellent catalytic properties of Ag@PM-*b*-B/GCE. When Ag@PM-*b*-B/GCE was stored at 4°C, further repeated tests about the stability of the sensor were carried out every ten days in one month. The remained current response to 100  $\mu\text{M}$  glucose is shown in Fig. 6B. The Ag@PM-*b*-B/GCE keeps at least 90% of the initial response in the continuous tests in one month, proposing the long-term stability of the electrode. The reproducibility of the sensor was also examined. Five different modified electrodes are established independently for the amperometric response of glucose, giving a relative standard deviation (R.S.D.) less than 7%. These results approve that the prepared sensor is highly reproducible and stable.

The effect of common interfering species on Ag@PM-*b*-B/GCE was studied. Fig. 6C shows the amperometric response of the modified electrode towards the successive addition of 100  $\mu\text{M}$  glucose and this is followed by ascorbic acid, ethanol, glycine and uric acid into 0.1 M NaOH

solution. As seen, the current of these interfering substances does not reveal an obvious additional signal which indicates that proposed sensor has a good selectivity towards glucose.

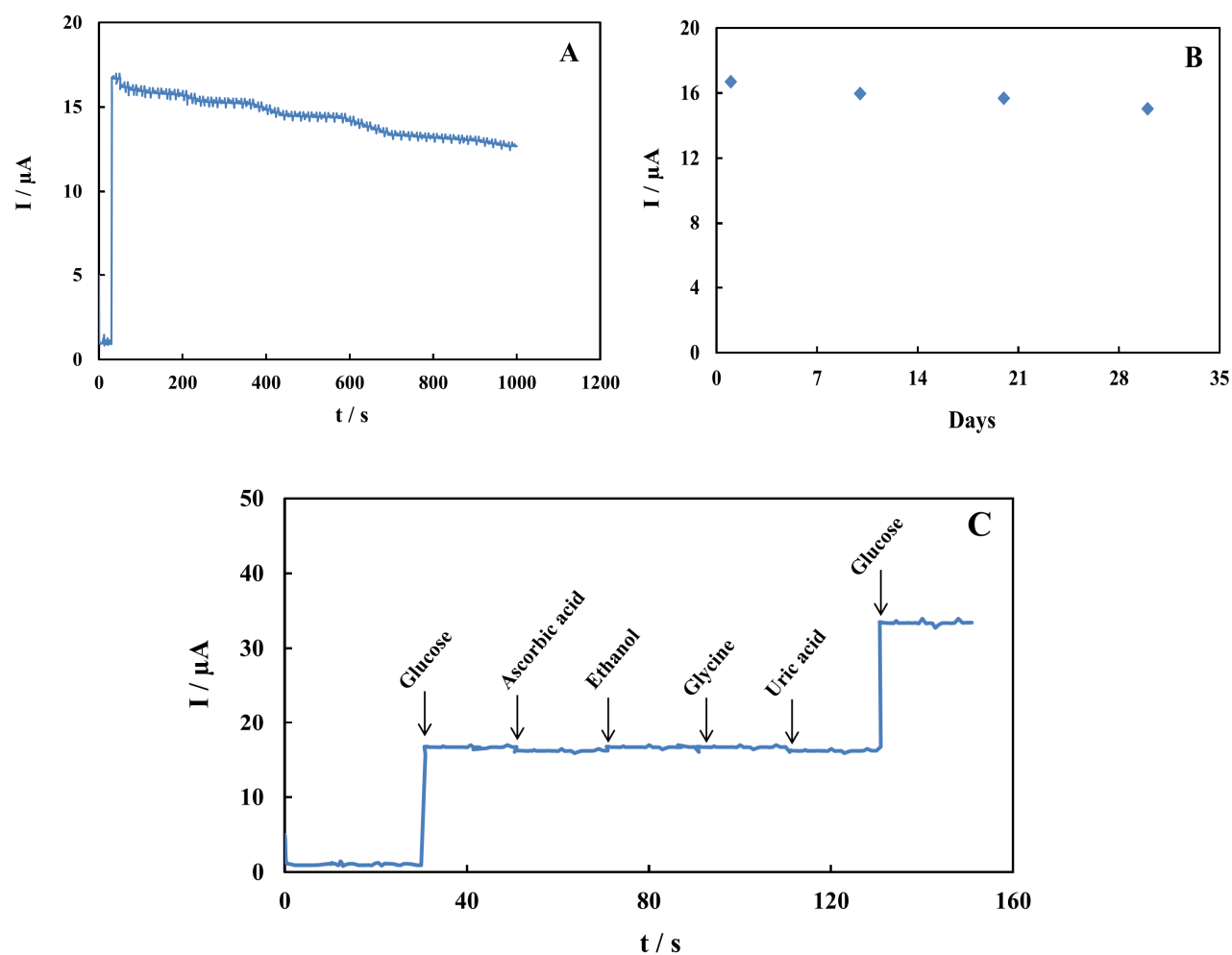


**Fig. 6.** (A) The amperometric response for the oxidation of 100  $\mu\text{M}$  glucose in 0.1 M NaOH solution at +0.7 V at the surface of Ag@PM-b-B/GCE. (B) Stability of the fabricated sensor to glucose tested every ten days by amperometric measurements in one month. (C) Amperometric response of Ag@PM-b-B/GCE upon the successive addition of glucose (100  $\mu\text{M}$ ), ascorbic acid (500  $\mu\text{M}$ ), ethanol (300  $\mu\text{M}$ ), glycine (300  $\mu\text{M}$ ) and uric acid (500  $\mu\text{M}$ ) into 0.1 M NaOH solution with an applied potential +0.7 V under a stirring condition.

## Experimental Section

All reagents were obtained from commercial sources and were used without purification. IR spectra were recorded as KBr pellets on a Shimadzu 435-U-04 spectrophotometer. SEM images were recorded on a Hitachi S4160 instrument. Electrochemical experiment including cyclic voltammetry (CV) was recorded with a Metrohm (797 VA Computrace, Switzerland) controlled by a personal computer. The measurements were carried out using a conventional three electrode cell using an Ag|AgCl|KCl (3 M) electrode as the reference and a Pt wire as the counter (auxiliary) electrode. A glassy carbon electrode with a geometrical area of 0.0314 cm<sup>2</sup>, bare or modified, was used as working electrode. <sup>1</sup>H and <sup>13</sup>C NMR spectra were determined on a Bruker DRX-300 Avance spectrometer in DMSO-d<sub>6</sub> or CDCl<sub>3</sub>, and shifts are given in δ downfield from tetramethylsilane (TMS) as an internal standard. Melting points were determined using an Electrothermal 9200 apparatus and are uncorrected.

### 1. General Procedure for the Synthesis of Symmetrical *N,N'*-Alkylidene *bis*-Amides

The catalyst, NiFe<sub>2</sub>O<sub>4</sub>@SiO<sub>2</sub>-PPA (0.1 g), was added to a mixture of the aldehyde (1 mmol), the amide (2 mmol), and 1 mL of methanol in a 5 mL flask fitted with a reflux condenser. The resulting mixture was heated to reflux (an oil bath) for the appropriate time (*see Table 2*) with stirring (spin bar). After the completion of the reaction as determined by TLC (*n*-hexane-ethyl acetate, 2:1), the nanomagnetic catalyst was separated from the reaction mixture by employing an external magnetic field. The resulting crude product was poured into crushed ice and the solid product, which separated was filtered and recrystallized from ethanol 96% (2 ml) to afford the pure symmetrical *N,N'*-alkylidene *bis*-amide (**3a-r**).



## 2. Preparation of Ag@PM-*b*-B modified GCE (Ag@PM-*b*-B/GCE)

The glassy carbon electrode (GCE) was first successively polished using alumina slurries, rinsed with doubly distilled water in ultrasonic bath for 3 min. Finally, the electrode was rinsed with 1:1 ethanol, 1:1 nitric acid, and doubly distilled water in ultrasonic bath, respectively. The cleaned GCE was dried at ambient temperature before the modification. 0.5 mg PM-*b*-B was sonicated in 1 mL distilled water to obtain white suspension. 10  $\mu$ L of the PM-*b*-B suspension was dropped on the surface of the clean GCE. After being dried in air, the PM-*b*-B functionalized GCE (PM-*b*-B/GCE) was immersed in the 1 mM AgNO<sub>3</sub> solution. The synthesis of Ag NPs was performed by the electrodeposition on the PM-*b*-B/GCE at 0.0 V for 120 s in 1 mM AgNO<sub>3</sub> solution (deaerated by bubbling with nitrogen).

### Analytical Data for Selected Compounds.

***N,N'*-(3-Bromophenylmethylene)dibenzamide (3j):** IR: 3280, 1675, 1540, 1510, 1480, 1330, 1280, 1080, 715, 690; <sup>1</sup>H NMR (300 MHz, DMSO-*d*<sub>6</sub>):  $\delta$  6.94 (t, 1H, CH), 7.31-7.42 (m, 6H), 7.51-7.60 (m, 5H), 8.09 (d, 2H), 7.82 (s, 1H), 7.94 (d, 2H, NH, D<sub>2</sub>O exchangeable); <sup>13</sup>C NMR (75 MHz, DMSO-*d*<sub>6</sub>):  $\delta$  59.31, 114.70, 127.65, 128.08, 128.71, 128.91, 129.91, 132.31, 133.72, 134.91, 159.31, 166.61.

***N,N'*-(3-Phenoxyphenylmethylene)dibenzamide (3m):** IR: 3310, 1705, 1580, 1540, 1480, 1340, 1210, 710; <sup>1</sup>H NMR (300 MHz, DMSO-*d*<sub>6</sub>):  $\delta$  6.91 (t, 1H, CH), 6.97-7.14 (m, 5H), 7.22-7.24 (d, 2H), 7.33-7.57 (m, 9H), 7.86-7.98 (d, 4H), 9.00 (d, 2H, NH, D<sub>2</sub>O exchangeable); <sup>13</sup>C NMR (75 MHz, DMSO-*d*<sub>6</sub>):  $\delta$  58.46, 116.49, 117.50, 118.71, 121.58, 123.54, 127.46, 128.28, 129.93, 129.99, 131.56, 133.73, 133.77, 142.53, 156.29, 156.70, 165.59, 165.67.

## Conclusion

In conclusion, NiFe<sub>2</sub>O<sub>4</sub>@SiO<sub>2</sub>-PPA, was found to be an efficient magnetically catalyst for the reaction aldehydes with amides to afford the corresponding product in high to excellent yields. These catalysts have several advantages over homogeneous acid catalysts; they are not corrosive, are environmentally benign, present fewer disposal problems, are removed easily and are thermally stable. The catalyst can be easily isolated from the reaction mixture by simple magnetic separation, and it can be used in six reaction cycles without any significant loss of activity. Furthermore, a new and facile Ag@PM-*b*-B nanocomposite electrochemical sensor was successfully developed for the detection of glucose, which used the advantages of the high conductivity, large specific surface area and excellent electrochemical activity of Ag NPs. The proposed sensor showed rapid electrochemical detection of glucose and will have the potential applications in clinical diagnostics and biotechnology.

**Acknowledgements.** The author thanks the Research Council of Hakim Sabzevari University for partial support of this work.

## References

1. P. V. Pallai, R. S. Struthers, M. Goodman, L. Moroder, E. Wunsch and W. Vale, *Biochem.*, 1985, **24**, 1993.
2. M. Rodriguez, P. Dubreuil, J. P. Bali and J. Martinez, *J. Med. Chem.*, 1987, **30**, 758.
3. E. E. Magat, F. Farisj, E. Reith and L. F. Salisbu, *J. Am. Chem. Soc.*, 1951, **73**, 1028.
4. A. H. Fernandez, R. M. Alvarez and T. M. Abajo, *Synthesis*, 1966, 1299.
5. N. P. Selvam, S. Saranya and P. T. Perumal, *Can. J. Chem.*, 2008, **85**, 32.

6. M. Anary-Abbasinejad, M. H. Mosslemin, A. Hassanabadi and S. Tajik Safa, *Synth. Commun.*, 2010, **40**, 2209.
7. M. R. Mohammad Shafiee, *Can. J. Chem.*, 2011, **89**, 555.
8. G. Harichandran, S. D. Amalraj and P. Shanmugam, *J. Iran. Chem. Soc.*, 2011, **8**, 298.
9. G. Harichandran, S. D. Amalraj and P. Shanmugam, *Indian J. Chem.*, 2011, **50B**, 77.
10. W. Hongshe and Z. Weixing, *Chin. J. Org. Chem.*, 2013, **33**, 1822.
11. M. R. Mohammad Shafiee, *J. Saudi Chem. Soc.*, 2014, **18**, 115.
12. M. R. Mohammad Shafiee, *Lett. Org. Chem.*, 2011, **8**, 562.
13. Z. Karimi-Jaberi and B. Pooladian, *Monatsh. Chem.*, 2013, **144**, 659.
14. B. F. Mirjalili and M. A. Mirhoseini, *J. Chem. Sci.*, 2013, **125**, 1481.
15. B. Maleki, F. Mohammadi Zonoz, H. A. Akhlaghi, *Org. Prep. Proced. Int.*, 2015, **47**, 361.
16. R. Yolanda de Miguel, *J. Chem. Soc. Perkin. Trans.*, 2000, **1**, 4213.
17. R. A. Sheldon and H. Van Bekkum, *Fine Chemicals through Heterogeneous Catalysis*, Wiley-VCH, Weinheim, 2001.
18. J. H. Clark, D. J. Macquarrie, *Green Chemistry and Technology*, Blackwell, Abingdon, 2002.
19. J. Ying, R. M. Lee, P. S. Williams, J. C. Jeffrey, S. F. Sherif, B. Brian and Z. Maciej, *Biotechnol. Bioeng.*, 2007, **96**, 1139.
20. J. Lee, Y. Jun, S. Yeon and J. Shin, *Angew. Chem. In. Ed.*, 2006, **45**, 8160.
21. N. Tobias, S. Bernhard, H. Heinrich, H. Margarete and V. R. Brigitte, *J. Magn. Mater.*, 2005, **293**, 483.
22. H. Gu, K. Xu, C. Xu and B. Xu, *Chem. Commun.*, 2006, **9**, 941.

23. I. Akira, T. Kouji, K. Kazuyoshi, S. Masashige, H. Hiroyuki, M. Kazuhiko, S. Toshiaki and K. Takeshi, *Cancer. Sci.*, 2003, **94**, 308.
24. (a) S. Sobhani and Z. Pakdin-Parizi, *RSC Adv.*, 2014, **4**, 13071; (b) V. Polshettiwar, R. Luque, A. Fihri, H. Zhu and M. Bouhrara, *Chem. Rev.*, 2011, **111**, 3036; (c) B. Maleki, S. Barat Nam Chalaki, S. Sedigh Ashrafi, E. Rezaee Seresht, F. Moeinpour, A. Khojastehnezhad and R. Tayebee, *Appl. Organometal. Chem.*, 2015, **29**, 290; (d) B. Maleki, M. Baghayeri, S. M. Vahdat, A. Mohammadzadeh and S. Akhoondi, *RSC Adv.*, 2015, **5**, 46545; (e) B. Maleki and S. Sedigh Ashrafi, *RSC Adv.*, **4**, 42873 (2014); (f) M. Baghayeri, H. Veisi, H. Veisi, B. Maleki, H. Karimi-Maleh and H. Beitollahi, *RSC Adv.*, 2014, **4**, 49595; (g) H. Veisi, A. Naeimi, B. Maleki, S. Sedigh Ashrafi and A. Sedrpoushan, *Org. Prep. Proced. Int.*, **47**, 309 (2015); (h) B. Maleki, H. Eshghi, A. Khojastehnezhad, R. Tayebee, S. Sedigh Ashrafi, G. Esmailian Kahoo, F. Moeinpour, *RSC Adv.*, 2015, **5**, 64850; (i) B. Maleki, H. Eshghi, M. Barghamadi, N. Nasiri, A. Khojastehnezhad, S. Sedigh Ashrafi, G. Esmailian Kahoo and O. Pourshiani, *Res. Chem. Intermed.*, DOI: 10.1007/s11164-015-2198-8 (2015); (j) R. Tayebee, M. Jarrahi, B. Maleki, M. Kargar Razi, Z. B. Mokhtari and S. M. Baghbanian, *RSC Adv.*, 2015, **5**, 10869; (k) S. Fernandes, C. M. Eichenseer, P. Kreitmeier, J. Rewitzer, V. Zlateski, R. N. Grass, W. J. Stark and O. Reiser, *RSC Adv.*, 2015, **5**, 46430; (l) J. Zhi, S. Mitchell, J. Pérez-Ramírez and O. Reiser, *ChemCatChem* 2015, **7**, 2544; (m) Q. M. Kainz and O. Reiser, *Acc. Chem. Res.*, 2014, **47**, 667; (n) A. S. Kumar, M. A. Reddy, M. Knorn, O. Reiser and B. Sreedhar, *Eur. J. Org. Chem.*, 2013, 4674; (o) M. Keller, A. Perrier, R. Linhardt, L. Travers, S. Wittmann, A.-M. Caminade, J.-P. Majoral, O. Reiser, A. Ouali, *Adv. Synth. Catal.*, 2013, **355**, 1748.

25. (a) G. Chouhan, D. S. Wang and H. Alper, *Chem. Commun.*, 2007, **45**, 4809; (b) E. Rafiee and S. Eavani, *Green Chem.*, 2011, **13**, 2116; (c) B. Maleki, S. Babae and R. Tayebee, *Appl. Organometal. Chem.*, 2015, **29**, 408; (d) M. Knorn, T. Rawner, R. Czerwiec and O. Reiser, *ACS Catal.*, 2015, **5**, 5186.
26. (a) X. X. Zheng, S. Z. Luo, L. Zhang and J. P. Cheng, *Green Chem.*, 2009, **11**, 455; (b) B. Maleki and S. Sheikh, *RSC Adv.*, 2015, **5**, 42997; (c) B. Maleki and F. Taimazi, *Org. Prep. Proced. Int.*, 2014, **46**, 252; (d) B. Maleki, E. Rezaee-Seresht and Z. Ebrahimi, *Org. Prep. Proced. Int.*, 2015, **47**, 149; (e) B. Maleki, *Org. Prep. Proced. Int.*, 2015, **47**, 173; (f) A. Mohammadi, H. Keshvari, R. Sandaroos, B. Maleki, H. Rouhi, H. Moradi, Z. Sepehr, S. Damavandi, *Appl. Catal. A: Gen.*, 2012, **329-330**, 73; (g) B. Maleki, D. Azarifar, R. Ghorbani-vaghei, H. Veisi, S. F. Hojati, M. Gholizadeh, H. Salehabadi, M. Khodaverdian Moghadam, *Monatsh Chem.*, 2009, **140**, 1485; (h) B. Maleki, S. Barzegar, Z. Sepehr, M. Kermanian and R. Tayebee, *J. Iran. Chem. Soc.*, 2012, **9**, 757.
27. (a) A. Kuchler, J. Adamcik, R. Mezzenga, A. D. Schlüter and P. Walde, *RSC Adv.*, 2015, **5**, 44530; (b) N. Gao, Y. L. Chen, Y. H. He and Z. Guan, *RSC Adv.*, 2013, **3**, 16850.
28. (a) T. Marimuthu, S. Mohamad and Y. Alias, *Synth. Met.*, 2015, **207**, 35; (b) C. Chen, Q. Xie, D. Yang, H. Xiao, Y. Fu, Y. Tan and S. Yao, *RSC Adv.*, 2014, **4**, 4473.
29. K. An and G. A. Somorjai, *ChemCatChem* 2012, **4**, 1512.
30. J. Dong, L. Ren, Y. Zhang, X. Cui, P. Hu and J. Xu, *Talanta*, 2015, **132**, 719.
31. M. Pan, G. Fang, Y. Lu, L. Kong, Y. Yang and S. Wang, *Sensor. Actuat., B* 2015, **207**, 588.
32. (a) B. Maleki, S. Hemmati, A. Sedrpoushan, S. Sedigh Ashrafi and H. Veisi, *RSC Adv.*, 2014, **4**, 40505; (b) H. Veisi, B. Maleki, M. Hamelian and S. Sedigh Ashrafi, *RSC Adv.*,

- 2015, 6365; (c) H. Veisi, B. Maleki, F. Hosseini Eshbala, H. Veisi, R. Masti, S. Sedigh Ashrafi and M. Baghayeri, *RSC Adv.*, 2014, **4**, 30683; (d) B. Maleki, S. Sedigh Ashrafi and R. Tayebee, *RSC Adv.*, 2014, **4**, 41521; (e) B. Maleki, E. Akbarzadeh and S. Babaei, *Dyes Pigm.*, 2015, **123**, 222; (f) B. Maleki and S. Sheikh, *Org. Prep. Proced. Int.*, 2015, **47**, 368; (g) B. Maleki, *Coll. Czech. Chem. Commun.*, 2011, **76**, 27; (h) B. Maleki, S. Hemmati, R. Tayebee, S. Salemi, Y. Farokhzad, M. Baghayeri, F. Mohammadi Zonoz, E. Akbarzadeh, R. Moradi, A. Entezari, M. R. Abdi, S. Sedigh Ashrafi, F. Taimazi and M. Hashemi, *Helv. Chim. Acta*, 2013, **96**, 2147.
33. A. Khojastehnezhad, M. Rahimizadeh, F. Moeinpour, H. Eshghi and M. Bakavoli, *C. R. Chim.*, 2014, **17**, 459.
34. W. Wang, Z. Li, W. Zheng, J. Yang, H. Zhang, C. Wang, *Electrochem. Commun.*, 2009, **11**, 1811.
35. L. Wang, Y. Zheng, L. Xingping, L. Zhuang, L. Sun, Y. Song, *Sens. Actuators B* 2014, **195**, 1.
36. X. Li, J. Yao, F. Liu, H. He, M. Zhou, N. Mao, P. Xiao, Y. Zhang, *Sens. Actuators B* 2013, **181**, 501.
37. J. Song, L. Xu, R. Xing, W. Qin, Q. Dai, H. Song, *Sens. Actuators B* 2013, **182**, 675.
38. C. Wang, L. Yin, L. Zhang, R. Gao, *J. Phys. Chem. C* 2010, **114**, 4408.